Journal of Materials Chemistry A

ROYAL SOCIETY OF CHEMISTRY

REVIEW

View Article Online
View Journal | View Issue

Cite this: J. Mater. Chem. A, 2023, 11, 11987

Opportunities and challenges of zinc anodes in rechargeable aqueous batteries

Xiaoxia Guo and Guanjie He *

Aqueous rechargeable zinc-ion batteries (ZIBs) have recently attracted increasing research interests due to their high safety, low cost, abundant resources, and eco-friendliness compared with commercial lithium-ion batteries. However, problems of zinc anodes in ZIBs such as zinc dendrites and side reactions severely shorten the cycling lifetime and restrict the practical application of ZIBs. In this review, the fundamental understanding of existing issues including dendrite formation, corrosion, and hydrogen evolution are mainly revealed, the current existing strategies on the protection of the zinc electrode and electrolyte engineering in the aqueous electrolyte are discussed. In addition, the existing techniques applied on analyzing the interaction between anodes and electrolytes are summarized. Furthermore, perspectives and suggestions are provided to design highly stable zinc anodes.

Received 31st March 2023
Accepted 22nd May 2023

DOI: 10.1039/d3ta01904g

rsc.li/materials-a

1. Introduction

Electrochemical energy storage systems, such as rechargeable batteries, can effectively alleviate the world's energy crisis.[1] Among various options, lithium-ion batteries (LIBs) with their inherent advantages, including high specific energy density (5928 W h kg^{-1}) and long cycling stability,[2–4] have been widely applied in portable electronics and considered promising for powering electric vehicles.[5] However, limited lithium resources, the high cost (~US$ 83 kg^{-1})[6] and underlying safety issues motivate the research for other battery systems beyond the LIB technology. As alternatives, battery systems based on more abundant elements, including naturally abundant alkali metal ions (Na^+ and K^+) and multivalent charge carriers (Zn^{2+}, Mg^{2+}, Al^{3+}, *etc.*), have received extensive attention.[7–9] Although Na and K elements are relatively abundant and have similar chemical properties to Li, non-aqueous sodium-ion batteries (SIBs) and potassium-ion batteries (KIBs) are also suffering from the low energy density (100–120 W h kg^{-1}, 150–170 W h kg^{-1}), highly toxic and flammable electrolytes, high operating cost and potential safety issues. As for magnesium-ion batteries (MIBs) and aluminum-ion batteries (AIBs), although they can theoretically achieve higher specific capacity and energy density due to multi-electron-involving redox reactions.[10,11] The available cathode materials for MIBs have been limited to very few compounds

Electrochemical Innovation Lab, Department of Chemical Engineering, University College London, Torrington Place, London, WC1E 7JE, UK. E-mail: g.he@ucl.ac.uk

Xiaoxia Guo received her master's degree (2018) from CSU and PhD (2023) from UCL with Dr Guanjie He and Prof. Ivan P. Parkin. During 2020–2022, she studied in Prof. Quanhong Yang's group at Tianjin University (TJU) as an exchange PhD student. She is carrying out her Postdoctoral Research in Department of Chemical Engineering at UCL since 2022. Her research interests include lithium-ion batteries and aqueous zinc-ion batteries.

Guanjie He is an Assistant Professor in the Department of Chemical Engineering in University College London (UCL). He received his PhD degree from UCL in 2018 and visited Yale University during the doctoral study. He has worked at Queen Mary University of London and the University of Lincoln. His research fields are mainly aqueous batteries, electrocatalytic materials and devices, advanced characterization, and simulation. He has received EPSRC New Investigator Award, ERC Starting Grant and STFC Early Career Awards, etc. due to his research on Zn-ion batteries.

Table 1 Zn property regimes: a comparison with other metal anodes

	Atomic mass	Standard potential (V *vs.* Standard Hydrogen Electrode, SHE)	Gravimetric capacity (mA h g^{-1})	Volumetric capacity (mA h cm^{-3})	Cost (\$ kg^{-1})
Li	6.94	−3.04	3860	2062	81.4–85.6
Na	23	−2.71	1166	1128	2.57–3.43
Zn	65.41	−0.76	820	5851	2.55
Mg	24.31	−2.36	2206	3833	2.32
Al	26.98	−1.67	2980	8046	4.84

owing to the sluggish Mg^{2+} diffusion in host lattices.[12] In addition, the passivation of the Mg anode greatly prevents further transport of Mg^{2+} ions.[13,14] AIBs are in the primary development stage because of the formation of Al_2O_3 layers on the anode, leading to the corrosion of aluminum electrodes, decrease of battery efficiency and low cycling stability.[15–17]

Among all available energy storage systems, rechargeable aqueous Zn-ion batteries (ZIBs) are considered as the most promising class of batteries for grid-scale storage due to their much lower cost (~US\$ 2.5 kg^{-1}), higher cycling stability, aqueous electrolytes, nontoxicity, and safe battery manufacturing process.[8,18,19] Table 1 shows the comparation of Zn and other metal anodes including Li. The biggest advantage of metallic Zn over Li, Na, and K is that the electrochemical redox voltages of metallic Zn are matched with the stable potential window of water, make it possible for metallic Zn to directly work as the anode in aqueous solutions.[20] In addition, the price of typical cathode materials for ZIBs such as MnO_2 (~ US\$ 1.7 kg^{-1}) and V_2O_5 (~US\$ 5.5 kg^{-1}) are much cheaper than that of LIBs (*e.g.* $LiCoO_2$, ~US\$ 55 kg^{-1} and Li(Ni, Mn, Co)O_2, ~US\$ 34 kg^{-1}).[7,8,21,22] Moreover, the generally used aqueous electrolyte for ZIBs is much cheaper with safer feature and higher ionic conductivity (0.1–6 S cm^{-1}) when compared to flammable organic electrolytes in LIBs (10^{-3} to 10^{-2} S cm^{-1}). Due to these advantages, ZIBs have promising prospects for practical applications.

The Zn metal was employed as an anode for the first battery invented in 1799, known as Voltaic Pile.[23] After which, the Zn was regarded as an ideal negative electrode in various primary and secondary Zn-based batteries, including Zn–MnO_2, Zn–Ni, Zn–Ag_2O, Zn–air and Zn-ion batteries, *etc*. At the first stage of the Zn-based battery, alkaline Zn–MnO_2 batteries showed great potential and dominated the primary battery application after their commercialization.[24] However, the commercial application of the Zn anode in rechargeable Zn-based batteries is hindered by the fast capacity decay and the low coulombic efficiency (CE), which is mainly due to the uncontrollable growth of Zn dendrites and the formation of irreversible discharge by-products (*e.g.*, ZnO) in alkaline electrolytes.[25] In this regard, aqueous Zn-ion batteries (ZIBs) with neutral (or slightly acidic) electrolyte hold particular promise for grid-scale energy storage application.

As shown in Fig. 1, a rechargeable ZIB generally consists of a metallic Zn anode, a Zn^{2+} host cathode and a salt electrolyte containing Zn^{2+}, operating *via* the reversible Zn^{2+} intercalation/deintercalation (cathode) and Zn plating/stripping (anode) upon discharge/charge processes.

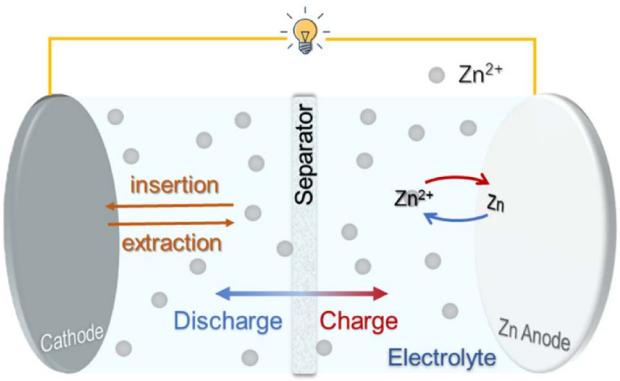

Fig. 1 Schematic illustration of the working principle of rechargeable Zn-ion batteries.

To date, extensive studies have been reported for ZIBs, covering metallic Zn anodes, cathode materials, electrolyte additives and potential applications. Recently investigated neutral and mildly acidic aqueous electrolytes are demonstrated to minimize the formation of Zn dendrites and inactive species that often appear in the alkaline media.[18,26] However, the CE of Zn plating/stripping, operating voltage and the full utilization of Zn anodes remain unsatisfactory.

Currently, numerous reviews on ZIBs merely focused on a specific component or device. But the optimization strategies of Zn anodes and the design of electrolyte, especially the organic electrolytes in ZIBs are lack of summarization. In this review, the basic properties and challenges of metallic Zn anodes are briefly introduced, followed by the discussion of the optimization strategies related to Zn anodes in both aqueous and organic solvents. We also review recent research on how to determine the significance of an electrolyte's solvation structure, construct an interfacial model to comprehend the electrode's performance, and apply these theories to the design of electrolytes. Finally, potential future research directions and different techniques are also summarized. This review provides a comprehensive overview focusing on the recent progress, challenges, and future perspectives of the modification of Zn anodes and electrolytes in aqueous ZIBs.

2. Fundamentals of the metal Zn as the anode

2.1 Zn as the anode

Metallic Zn is the most widely used anode material for aqueous batteries because of its high abundance, low cost,[27] high

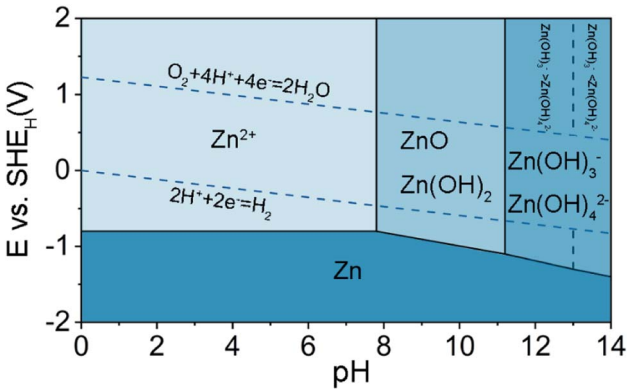

Fig. 2 The Pourbaix diagram of Zn in aqueous solution.

theoretical specific capacity (gravimetric and volumetric capacities of 820 mA h g^{-1} and 5855 mA h cm^{-3}, respectively),[28] environmental friendliness, suitable redox potential (−0.76 V *vs.* SHE) as well as good reversibility in the aqueous electrolyte.[29–31]

Generally speaking, the electrochemical behaviors associated with the Zn electrode are also highly correlated with the pH of the electrolyte. It is better to understand the fundamental electrochemical reaction occurring on the Zn electrode with the Pourbaix diagram of Zn in aqueous environment, as shown in Fig. 2.[32] The diagram shows that the Zn can be oxidized to dissolved forms of Zn^{2+}, $Zn(OH)_2$, $HZnO^{2-}$, and ZnO_2^{2-} with the increase of the pH value in aqueous solutions.[33] The notations of $HZnO^{2-}$ and ZnO_2^{2-} correspond to Zn complexes of $Zn(OH)^{3-}$ and $Zn(OH)_4^{2-}$ in most cell equations. When pH < 4.0, Zn has a high solubility and can be easily dissolved as Zn^{2+}. At 5.0 < pH < 8.0, compared with strong acid solution, the dissolution of Zn becomes relatively slower due to the high overpotential and the lower corrosion activity. Under slightly alkaline solutions (8.0 < pH < 10.5), irreversible byproducts are generated during the charge/discharge process on the surface of Zn anodes (*e.g.*, ZnO, $Zn(OH)_2$). At pH > 11, Zn solubility decreases again and zincate ions (*e.g.*, $Zn(OH)_4^{2-}$) start to appear.

2.2 Challenges for Zn anodes

As mentioned above, Zn metal can be directly used as the anode. Most of studies in ZIBs employ commercial Zn foil as the anode for the investigation of ZIBs. However, the commercial application of the Zn anode is mainly hindered by following problems. Fig. 3 demonstrate the common problems occurring on Zn surfaces which include: (1) dendrite growth, (2) hydrogen evolution, (3) corrosion, and (4) passivation (in alkaline electrolyte).

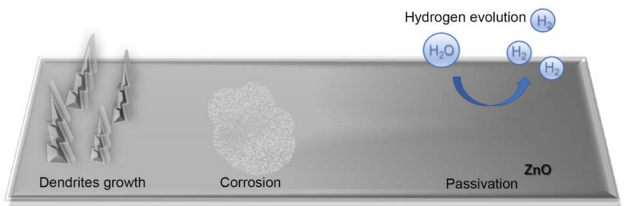

Fig. 3 Schematic illustration of possible reactions associated with Zn electrode in aqueous solution.

The Zn dendrite is serious especially in aqueous electrolyte, non-uniform Zn^{2+} dissolution and the uneven deposition of Zn occur on the electrode surface. It is easier for an incoming zinc atom to deposit on an existing stable nucleus than on a flat surface to form a new stable nucleus, due to the overpotential required for stable nuclei to grow in size will be smaller than that of the nucleation step. The sharp tips can act as a charge center in the electric field, further facilitating the growth of dendrites.[34] In addition, under aqueous condition, the discharge product $Zn_4SO_4(OH)_6\cdot xH_2O$ layer can be easily formed on the Zn surface, which decrease the surface contact between the electrolyte and the Zn anode, lower the utilization of Zn active materials and seriously increase the internal resistance of the anode.[35,36]

Hydrogen evolution reaction (HER) is a common side reaction in aqueous ZIBs, determined by thermodynamics. The standard reduction potential of Zn^{2+}/Zn (−0.76 V *vs.* SHE) is lower than that of HER according to the Pourbaix diagram in the entire pH range of 1–14, suggesting that the HER is more thermodynamically favorable than Zn deposition (Fig. 2). Although a large overpotential for the HER on Zn can suppress its kinetics, the hydrogen gas can still be gradually generated and accumulated in the cells. The cathodic reactions that occur on Zn electrodes during the charging of the cell include:

$$\text{Zn deposition: } Zn^{2+} + 2e^- \rightarrow Zn \quad (1)$$

$$\text{HER: } 2H_2O + 2e^- \rightarrow 2OH^- + H_2 \text{ (neutral or alkaline electrolytes)} \quad (2)$$

$$2H + 2e^- \rightarrow H_2 \text{ (acidic electrolytes)} \quad (3)$$

which means a Zn electrode cannot be charged with 100% CE as the electrons are partially consumed by HER. Even worse, the hydrogen gas will increase the internal pressure and cause battery swelling, resulting in battery failure in sealed systems.

Zn corrosion is another critical problem of ZIBs with mildly acidic electrolytes.

Although the formation of dendritic Zn could be alleviated in neutral pH (or slightly acidic) electrolyte,[37] the poor reversibility and low plating/stripping CE of the Zn anode still challenge its practical application. To overcome these problems, many efforts have been devoted to morphology tailoring of the Zn anode with the surface modification, designing the composite nanostructure of the Zn-based anodes, inducing additives or modification of the electrolytes, or changing the concentration of Zn salts in the electrolytes.

3. Typical stabilization strategies

3.1 Artificial protective layer

3.1.1 Surface modification. The passivation layer and the dendrite growth on the surface of Zn anodes could be

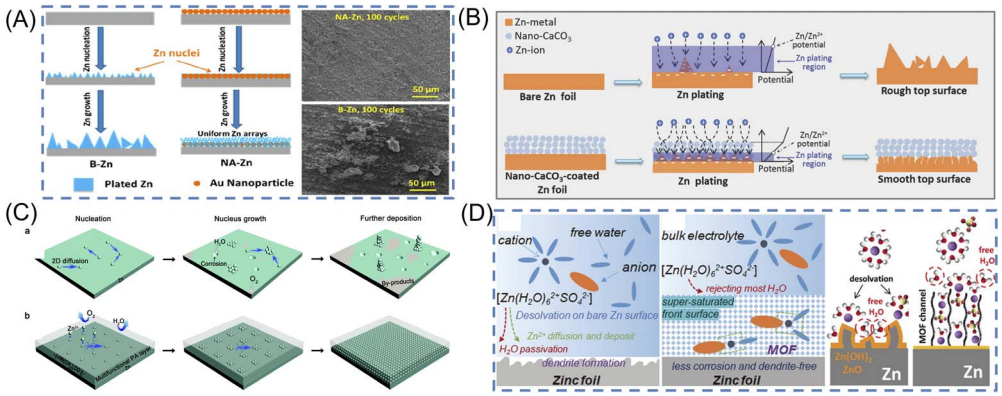

Fig. 4 Schematic diagrams of the designed surface coating layers. (A) Schematic illustration of the Zn stripping/plating process on B–Zn and NA–Zn anode and SEM images of B–Zn and NA–Zn after 100 cycles. Reproduced with permission.[72] Copyright 2019, American Chemical Society. (B) Schematic illustrations of morphology evolution for bare and nano-$CaCO_3$-coated Zn foils during Zn stripping/plating cycling processes. Reproduced with permission.[62] Copyright 2018, WILEY-VCH. (C) Schematic diagrams for bare Zn foils with corrosion, by-products and Zn dendrites from rampant 2D diffusion, and the PA layer for the dense and dendrite-free deposition morphology by refining the nucleus size, increasing the nucleus density resulting from constraining the 2D mass diffusion, and inhibiting the permeation of O_2 and H_2O. Reproduced with permission.[39] Copyright 2019, Energy & Environmental Science. (D) Schematic illustration of the surface evolution of bare Zn and the function mechanism of the MOF coating layer to reject H_2O and construct a super-saturated front surface. Reproduced with permission.[73] Copyright 2020, WILEY-VCH.

suppressed in acidic electrolytes,[38] but acidic electrolytes will cause the corrosion on Zn anodes, leading to an unstable long-term cyclability. Surface coating is the most direct way to protect the metal anodes, *via* preventing the direct contact of the Zn with the electrolyte from dendrite issues, normally prepared by doctor blading,[39] spin coating,[40] and atomic layer deposition.[41] However, in a battery system, it is essential to keep effective contact and migration pathways between the electrode and the electrolyte. Therefore, an ideal layer for Zn anodes should effectively isolate the Zn electrodes from the aqueous electrolyte and have sufficient transmission channels of Zn^{2+} cations. Various coating materials, including metallic compounds,[42–52] carbon-based materials,[39,53–61] and inorganic compounds including polymer materials[39,62–71] have been published.

Metal nanoparticles have been investigated for Zn metal anode surface coating due to their excellent anticorrosion properties and effectiveness in reducing Zn nucleation energy. By sputtering Au nanoparticles onto the Zn anode surface, preformed seeds are created that enable a uniform and stable Zn plating/stripping process (Fig. 4A).[72] Comparing the Au–Zn electrode to bare Zn foil, the Au–Zn electrode exhibits a relatively uniform surface morphology after cycling (electrolyte: 3 M $ZnSO_4$). Additionally, Cai *et al.* have successfully coated Zn metal with Cu nanoparticles using 0.1 M $CuCl_2$ as a precursor solution.[74] The improved stability of the Cu/Zn anode is due to the excellent corrosive resistance and positive electrode potential of Cu, which is electrochemically converted to a Cu–Zn alloy/Zn composite during cycling (electrolyte: 3 M $ZnSO_4$). Table 2 lists different metal nanoparticles that have been coated onto Zn anodes. Metal nanoparticles provide homogeneous surface electrical fields due to their superior electrical conductivity. Some metals also possess anticorrosion properties that can inhibit Zn metal in aqueous electrolytes. As seed layers on the surface of the Zn anode, metal nanoparticles could facilitate easier zinc nucleation. Furthermore, the interaction between metal and Zn atoms can facilitate Zn plating by providing several nucleation sites. As a result of these merits, metal nanoparticle-coated Zn anodes demonstrate high reversibility during the stripping/plating process.

To ensure the mass migration path in the inorganic coating layer, Liang *et al.* developed a simple strategy to improve the stripping/plating stability of Zn metal anodes *via* a nanoporous $CaCO_3$ coating.[62] As shown in Fig. 4B, the porous coatings confined the Zn plating reaction to the surface region of Zn foils, and guided uniform electrolyte flux and Zn plating rate over the entire Zn foil surface, resulting in a uniform, bottom-

Table 2 Summary of metal nanoparticles (NP) as coating materials for Zn anodes

Metal NPs	Overpotential	Condition	Cycling life	Ref.
Au	100 mV	0.25 mA cm^{-2}, 0.05 mA h cm^{-2}	2000 h	72
Cu	30 mV	1 mA cm^{-2}, 0.5 mA h cm^{-2}	1500 h	74
Cu	50 mV	0.1 mA cm^{-2}, 1 mA h cm^{-2}	5000 h	75
In	54 mV	0.2 mA cm^{-2}, 0.2 mA h cm^{-2}	1500 h	76
In	15 mV	0.25 mA cm^{-2}, 0.05 mA h cm^{-2}	1400 h	77
Sn	25 mV	1 mA cm^{-2}, 0.5 mA h cm^{-2}	500 h	78
Ag	25 mV	0.25 mA cm^{-2}, 0.25 mA h cm^{-2}	1500 h	79

up Zn plating behavior, thus effectively avoiding the corrosion and the growth of large protrusions/dendrites. Compared with the one using bare Zn anodes, the Zn||$ZnSO_4$ + $MnSO_4$|| carbon nanotubes (CNTs)/MnO_2 battery with a nano-$CaCO_3$-coated Zn anode delivers a 42.7% higher discharge capacity (177 *vs.* 124 mA h g^{-1} at 1 A g^{-1}) after 1000 cycles (electrolyte: 3 M $ZnSO_4$ + 0.1 M $MnSO_4$). To obtain highly ordered protecting layer, ALD technique was used to realize ultrathin (8 nm) TiO_2 coating on Zn anodes.[80] This coating of TiO_2 serves as a stable passivation layer for Zn metal, avoiding the direct contact between the Zn plate and the electrolyte and suppressing Zn corrosion process and hydrogen evolution. Additionally, the protection of TiO_2 extended the Zn||MnO_2 battery cycling performance up to 1000 cycles with the capacity retention of 85% (electrolyte: 3 M $Zn(SO_3CF_3)_2$ + 0.1 M $Mn(SO_3CF_3)_2$).

Carbon-based materials such as graphene,[59,60,81] CNTs,[61,82] carbon black[57] and activated carbon[54] are also applied to coat on the Zn surface due to their high electrical conductivity, good mechanical performance and chemical stability. For instance, using a Langmuir–Blodgett method, Chen *et al.* reported an artificial interface film of nitrogen (N)-doped graphene oxide (NGO) is one-step synthesized to create a parallel and ultrathin interface modification layer ($\approx$120 nm) on the Zn foil.[81] Due to the parallel graphene layer and the zincophilic-traits of the N-doped groups, the directional deposition of Zn crystals in the (002) planes is revealed. Additionally, *in situ* differential electrochemical mass spectrometry and *in situ* Raman tests show that the directional plating morphology of metallic Zn at the interface effectively suppresses HER and passivation. Consequently, the energy density of pouch cells paired with this new anode and $LiMn_2O_4$ cathode remains exceptional (164 W h kg^{-1} after 178 cycles) at a reasonable depth of discharge, 36% (electrolyte: 2 M $ZnSO_4$).

Another strategy to protect Zn anode is polymer layers on the Zn anode. Due to their abundant functional groups, such as C=O and N–H, polymers can provide absorption/coordination sites and transport Zn^{2+} to the reaction interface along the polymer chains. This modulates the uniform distribution of Zn^{2+} and improves cycling stability. Cui *et al.* designed a polyamide(PA)/$Zn(TfO)_2$ coating layer, the possession of amide groups that can coordinate with Zn^{2+}, elevate the nucleation barrier and restrict 2D diffusion of Zn^{2+} (Fig. 4C).[39] This hydrophilic PA interphase also suppresses free water/O_2-induced corrosion and passivation, and devotes to an ultra-long lifespan of the symmetric cells for more than 8000 hours (electrolyte: 2 M $ZnSO_4$ + 0.1 M $MnSO_4$). In another work, an even and dense polyvinyl butyral (PVB) SEI film was deposited on the surface of the Zn metal using the spin-coating method.[69] Benefiting from the abundant polar functional groups of the PVB chains, this insulating polymer shows good hydrophilicity and ionic conductivity, inhibiting the side reactions and Zn dendrite growth. The side-reaction-free and dendrite-free PVB@Zn anode facilitated repeated plating/stripping over 2200 h in the symmetric Zn cell, much longer than that of the bare Zn cells (electrolyte: 1 M $ZnSO_4$). A robust and lightweight poly(3-sulfopropyl methacrylate potassium salt) (PSPMA) molecular brush-grafted interface is constructed *via* a facile photo-initiated surface radical polymerization strategy for high-efficiency and dendrite-free Zn metal anodes.[83] The interface affords dense sulfo-terminated nanochannels as a powerful ion-redistributor to navigate fast and homogeneous Zn^{2+} flux and deposition with boosted transference number and reduced desolvation barrier energy of hydrated Zn^{2+}. As a consequence, the as-designed PSPMA@Zn anode delivers high coulombic efficiency of up to 99.9% for 900 cycles and ultralong Zn plating/stripping lifetime over 2500 h under a high current density of 10 mA cm^{-2} (electrolyte: 2 M $ZnSO_4$).

In addition, a metal–organic framework (MOF) was constructed as a front surface layer to maintain a super-saturated electrolyte layer on the Zn anode (Fig. 4D). The coating layer was found to avoid large-size solvated ion complexes, resulting in less water passivation and less byproduct accumulating on the Zn surface.[73] Benefiting from the unique super-saturated front surface, symmetric Zn cells survived up to 3000 hours at 0.5 mA cm^{-2} bare Zn anodes (electrolyte: 2 M $ZnSO_4$). An *in situ* anchoring of the Zn–phytic acid (PA) interphase on the Zn anode enables strong endurance on mechanical deformation and volume changes upon electrochemical plating/stripping.[84] More notably, the zincophilic Zn–PA interphase could navigate fast and dendrite-free Zn deposition by regulating the Zn^{2+} flux with a high Zn^{2+} transference number, low Zn^{2+} desolvation energy, and homogeneous interfacial electric field distribution. Parasitic side reactions are substantially suppressed to realize improved coulombic efficiency of 99.9%. Impressively, the Zn–PA@Zn anode delivers an ultralong lifetime of over 1700 h at 5 mA cm^{-2} with reduced nucleation/growth overpotentials and a superhigh cumulative plated capacity of 4.25 Ah cm^{-2} (electrolyte: 2 M $ZnSO_4$).

3.2 Host frameworks

3.2.1 Structured electrodes. In addition to the modification on 2D Zn surfaces, the fabrication of 3D composite nanostructures with the Zn anode is also an effective strategy to enhance the Zn anode performance by increasing exposed surfaces, shortening the ion transport paths, and relaxing the strain generated during battery cycling processes.[85] The plenty of research studies have been implemented to design advanced 3D Zn anodes, conductive substrates such as carbon cloths (CC),[86,87] graphite felt wafers,[88] 3D CNT[89] and porous copper skeletons[90,91] have been employed as light-weight backbones.

Wang *et al.* deposited Zn on conductive graphite felt by a simple electrodeposition method.[88] The graphite felt substrate can enhance cycling stability of Zn anodes due to the fast electron transport and the efficient Zn plating in various specific directions. A flexible 3D CNT framework with a high specific surface area and good electrical conductivity is applied as the Zn host to diminish the formation of dendrite, shown in Fig. 5A.[89] By introducing double-layer hydroxides to the preparation of the negative electrode, it can improve the plating/stripping CE of Zn anodes from 85 to 98% (electrolyte: 0.5 M $ZnSO_4$). This improvement was devoted to the elimination of a potential drop at the initial step of the Zn^{2+} reduction, avoiding the formation of H_2 during the discharge process.[93]

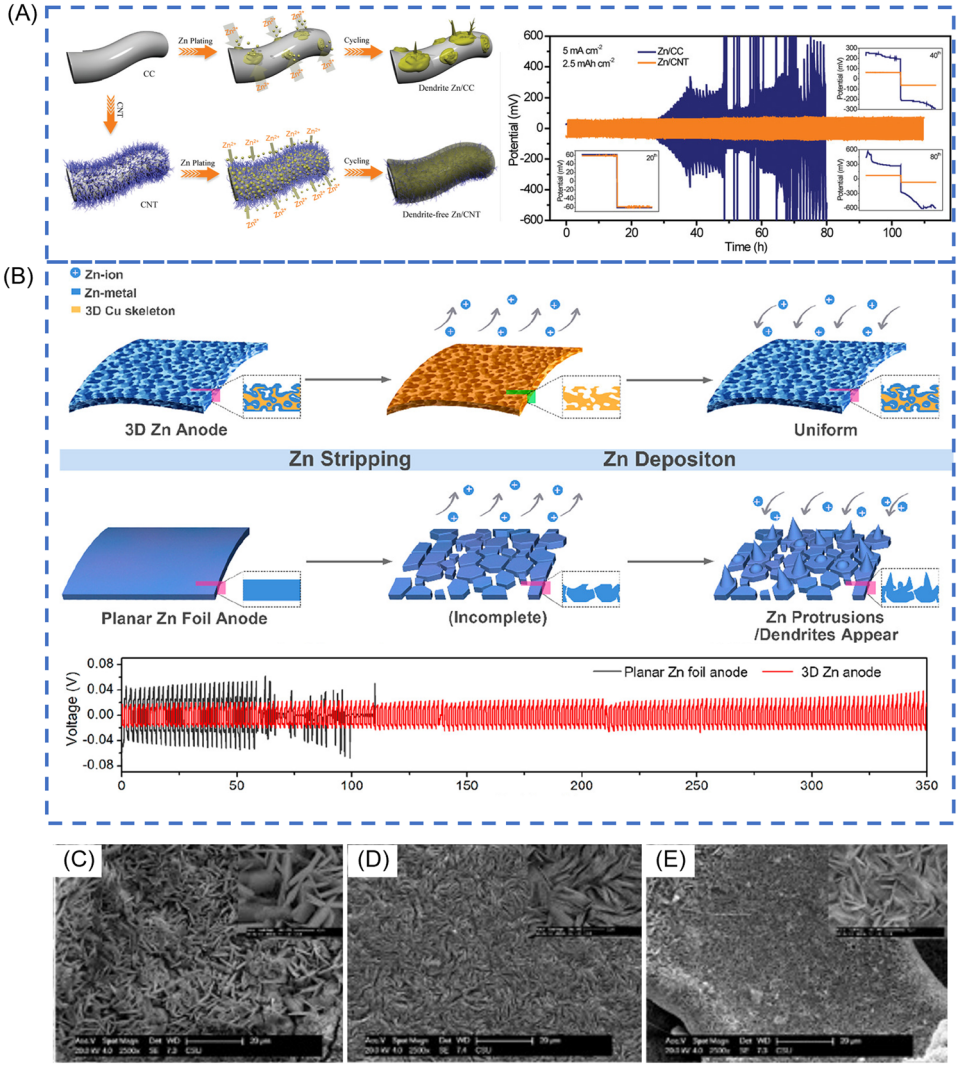

Fig. 5 (A) Schematic illustrations of Zn deposition on CC and CNT electrodes. Voltage profiles of symmetric cells based on Zn/CC and Zn/CNT anodes at 5 mA cm^{-2}. Reproduced with permission.[89] Copyright 2019, WILEY-VCH. (B) The schematic diagram of Zn deposition/stripping processes on 3D Zn electrodes and planar Zn foil electrodes. Cycling performance at a constant current of 0.5 mA cm^{-2} (the amount of Zn deposited in each cycle is 0.5 mA h cm^{-2}). Reproduced with permission.[92] Copyright 2019, American Chemical Society. SEM images of (C) Cu foam@Zn (D) Cu foil@Zn E. Ni foam@Zn after 10 cycle in discharge states. Reproduced with permission.[91] Copyright 2020, Elsevier.

Besides, the reversible epitaxial electrodeposition of Zn is attained by selecting a graphene-based substrate.[31] In contrast to the deposition morphology on stainless steel, in which Zn platelets are randomly oriented, Zn deposits formed on graphene with a low lattice mismatch are well directed, rendering cyclability over thousands of cycles (CE > 99% over 1000 cycles) (electrolyte: 2 M $ZnSO_4$). The substrate effect offers plenty of room to guide the nucleation and deposition of Zn for a stable structure.

Except for carbon substrate, alloys can improve the performance of Zn anodes. Lamella-nanostructured eutectic Zn–Al alloys have been reported to guide Zn^{2+} electrodeposition and protect against irreversible byproducts of ZnO or $Zn(OH)_2$, providing a stable and dendrite-free Zn plating/stripping behaviour.[42] Interestingly, preparing stable Zn anodes by electrodepositing Zn on chemically etched 3D porous copper skeletons ensured the uniform deposition of Zn and reached almost 100% CE due to the excellent electrical conductivity and open structures (Fig. 5B) (electrolyte: 2 M $ZnSO_4$).[92] Besides the 3D copper skeletons, other 3D metal skeletons can also be used as current collectors to construct 3D stable Zn anodes. Zhou and co-workers designed three novel 3D anodes by electroplating Zn on different substrates (copper foam, copper foil, and Ni foam), namely, Cu foil@Zn, Ni foam@Zn, and Cu foam@Zn (Fig. 5C–E). They found that Cu foam@Zn exhibits small voltage hysteresis, high CE and negligible self-discharge.[91] This should be attributed to the three-dimensional porous architecture, superb electrical conductivity and good corrosion resistance of Cu foam@Zn anode, guaranteeing its faster electrochemical kinetics, more uniform Zn deposition and stable cyclability.

4. Electrolyte and additives

4.1 Zinc salts

As an important component of ZIBs, the electrolyte plays a vital role in the electrochemical properties of ZIBs since it will provide a pathway for the migration of the Zn ions between the cathode and the anode, and determine the electrochemically stable potential window (ESPW), the reversibility of Zn plating/stripping processes, the reaction mechanisms, and the ionic conductivity. Compared with organic electrolyte, the aqueous electrolyte is popular in the research of ZIBs due to the unique advantages, including low cost, high safety, good ion conductivity, and environmental friendliness. But Zn is an amphoteric metal that can react with both OH^- or H^+ ions. In the aqueous electrolyte, Zn^{2+} ions interact strongly with water molecules, resulting in high energy barriers for solvated Zn^{2+} ions to desolvate and deposit. The generation of OH^- *via* the water decomposition often drives the formation of $Zn(OH)_2$, which further converts into insoluble $Zn_4SO_4(OH)_6 \cdot xH_2O$ and becomes electrochemically inactive. The large amount of OH^- in the conventional alkaline electrolyte can easily react with Zn to form byproducts, leading to rapid capacity decay and low CE (<50%). In contrast, with a small amount of H^+, the mildly acidic electrolytes can effectively alleviate the formation of byproducts, so neutral or mildly acidic aqueous electrolytes are more suitable for ZIBs. However, Zn anodes and current collectors will be corroded by acidic electrolytes. To solve this problem, many research efforts have been focused on the electrolyte optimization by adding functional additives in the electrolyte. Up to now, various Zn salts, such as oxidative Zn salts (*e.g.*, $Zn(NO_3)_2$, $Zn(ClO_4)_2$), Zn halides (*e.g.*, $ZnCl_2$, ZnF_2), Zn sulfate ($ZnSO_4$), zinc tetrafluoroborate hydrate ($Zn(BF_4)_2 \cdot nH_2O$) and organic Zn salts zinc trifluoromethane-sulfonate ($Zn(CF_3SO_3)_2$), zinc acetate ($Zn(CH_3COO)_2$), and zinc(II) bis(trifluoromethanesulfonyl)imide ($Zn(TFSI)_2$) were used to prepare ZIB electrolytes and show distinctive electrochemical properties.[20]

The aqueous $Zn(NO_3)_2$ solution (20 mM) was introduced in an aqueous Zn/copper hexacyanoferrate (CuHCF) battery. However, it is noted that the NO_3^- anions are strong oxidants and could corrode the electrodes, leading to serious corrosion of Zn foils and CuHCF cathode materials.[94]

The $Zn(ClO_4)_2$ solution shows a higher overpotential, which causes by the formation of by-products (*e.g.*, a ZnO thin layer on the Zn foil),[95,96] and the $ZnCl_2$ electrolyte show a narrow anode potential window ($\approx$0.75 V for 1 M $ZnCl_2$ solution),[87,97] both of them are not suitable as ideal electrolytes in ZIBs. As for ZnF_2, its application is limited by the low solubility of 86 mM in water.[96]

Currently, mildly acidic $ZnSO_4$ aqueous electrolyte exhibits excellent electrochemical stability in a wider electrochemical window. It is worth noting that the Zn anode has high dissolution/deposition reaction kinetics, slight dendritic growth, and weak corrosions in mild $ZnSO_4$ electrolytes.[98] However, its practical application is hampered by the HER and byproduct formation, which can reduce the Zn stripping/plating cycling stability and CE.[99]

Chen and co-workers firstly demonstrated that the bulky-anion Zn salts, $Zn(CF_3SO_3)_2$, offer an alternative option for high-performance ZIB constructions.[97] Specifically, the $Zn(CF_3SO_3)_2$ contributes to a smaller potential hysteresis between Zn^{2+} plating and stripping. The CE of $Zn(CF_3SO_3)_2$ electrolyte gradually increased and reached 100% after the third cycle in Fig. 6 (electrolyte: 3 M $Zn(CF_3SO_3)_2$). The spinel/carbon hybrid exhibits a reversible capacity of 150 mA h g^{-1} and a capacity retention of 94% over 500 cycles at a high rate of 500 mA g^{-1}. This is because the bulky CF_3SO^{3-} anions reduce the coordination number of H_2O molecules around Zn^{2+} and mitigate the solvation effect, facilitating Zn^{2+} transportation and charge transfer.[100] However, the cost of $Zn(CF_3SO_3)_2$ is almost 18 times higher than that of $ZnSO_4$, which restrains the application in large-scale storage system. Yang and co-workers proposed a hydrated $Zn(BF_4)_2$ salt and an ethylene glycol solvent (electrolyte: 4 m $Zn(BF_4)_2$/EG), which not only promotes the *in situ* formation of a favourable ZnF_2 passivation layer to protect Zn from dendrite growth and side reactions but also embraces excellent non-flammability.[101]

4.2 Electrolyte additives

Additives in electrolytes can change the surface properties of Zn anodes through adsorbing on the Zn electrode surface, shielding charge, or complexing with metal ions. As for the $ZnSO_4$ electrolyte, the additive for dendrite suppression can be mainly divided into organic and inorganic candidates, such as branched polyethyleneimine (BPEI), cetyltrimethylammonium bromide (CTAB), poly(ethylene glycol) (PEG), sodium dodecyl sulfate (SDS), thiourea and inorganic salts such as Na_2SO_4, $MnSO_4$, $Mn(CF_3SO_3)_2$, and $Ni(CF_3SO_3)_2$.[18,19,103–111] Organic additives can absorb on the Zn surface during electroplating and change the surface states of the anode, which may alter the crystallographic/morphological properties of the Zn surface. They are capable of functioning as the 2D host with a locked crystallographic orientation, contributing to the suppression of Zn dendrite growth. Among them, polymers are notable for their extensive range and adaptable molecular weight, effectively inhibiting the Zn dendrite formation on the anode surface. Liu *et al.* have utilized long-chain polyethylene oxide (PEO) as an electrolyte additive in $ZnSO_4$ electrolytes to stabilize the Zn metal anode.[112] The PEO molecules interact with the ether groups and Zn^{2+} ions, regulating Zn^{2+} ion transfer kinetics and concentration adjacent to Zn anodes. This regulates Zn^{2+} ion concentration distribution and electrolyte flux at the electrode/electrolyte interface, thereby suppressing Zn^{2+} ion transfer kinetics and achieving uniform Zn deposition–dissolution processes. The resulting Zn||$LiMn_2O_4$ full cells also demonstrate significantly enhanced cycling stability and higher CE (99%) in electrolytes containing PEO polymer (electrolyte: 1 M $ZnSO_4$ electrolyte with 0.5 wt% PEO). As for the inorganic additives, the selection of the additives mainly depends on the cathode materials and the Zn salts. Recently, ammonium dihydrogen phosphate (NHP), is introduced to regulate uniform zinc deposition and to suppress side reactions.[106] The results show that the NH^{4+} tends to be preferably absorbed on the Zn

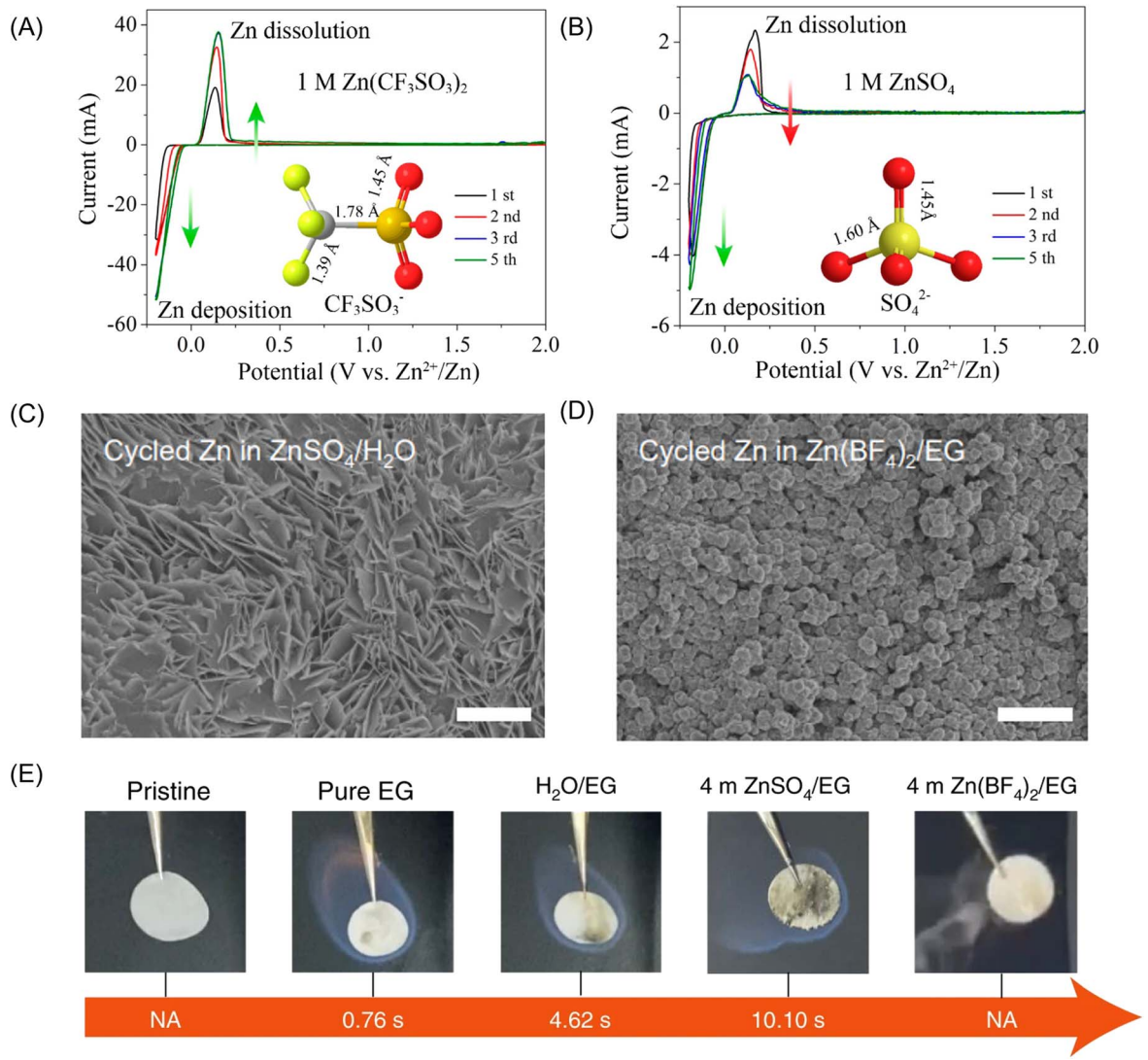

Fig. 6 Cyclic voltammetry of the Zn electrode in aqueous electrolyte of (A) 1 M $Zn(CF_3SO_3)_2$ and (B) 1 M $ZnSO_4$ at the scan rate of 0.5 mV s^{-1} between −0.2 and 2.0 V. Reproduced with permission.[102] Copyright 2016, American Chemical Society. Top-view SEM images of the cycled Zn after 20 cycles in (C) the reference aqueous $ZnSO_4$ electrolyte and (D) the 4 m $Zn(BF_4)_2$/EG electrolyte. (E) Ignition tests of a pristine glass fibre separator, one saturated with pure EG, a H_2O/EG solution, a 4 m $ZnSO_4$/EG solution and a 4 m $Zn(BF_4)_2$/EG solution. NA (not applicable) indicates non-flammability. Reproduced with permission.[101] Copyright 2021, Springer Nature.

surface to form a "shielding effect" and blocks the direct contact of water with Zn. Moreover, NH^{4+} and $(H_2PO_4)^-$ jointly maintain pH values of the electrode–electrolyte interface. Consequently, the NHP additive enables highly reversible Zn plating/stripping behaviors in Zn||Zn and Zn||Cu cells. Moreover, it has been demonstrated that Mn^{2+} in the electrolyte not only avoids the dissolution of MnO_2, but also effectively improves the CE of the Zn electrode, and thus enhance the cyclability of MnO_2 (electrolyte: 1 M $ZnSO_4$ + 0.1 M $MnSO_4$ + 25 mM NHP).[19]

4.3 Highly concentrated electrolyte

Highly concentrated neutral Zn-ion electrolyte with reduced free solvent molecules provides a promising way to suppress the dendrite growth and stabilize Zn electrodes. To completely eliminate the formation of Zn dendrites, Wang *et al.* developed a high-concentration electrolyte composed of 1 M $Zn(TFSI)_2$ and 20 M LiTFSI, achieving nearly 100% CE and no dendrite formation during Zn plating/stripping, shown in Fig. 7(C and D).[25] Similar to $Zn(CF_3SO_3)_2$, in such a highly concentrated electrolyte, the surrounding of Zn^{2+} ions is occupied primarily by $TFSI^-$ instead of H_2O, which effectively prevents H_2 evolution and the formation of $(Zn\text{-}(H_2O)_6)^{2+}$. In another work, Zhang *et al.* report a 30 m $ZnCl_2$,[30] which enables a dendrite-free Zn metal anode to possess a high CE. The Zn^{2+} solvation structure were converted to $[ZnCl_4]^{2-}$, inhibiting the formation of $Zn(OH)_2$ and ZnO. In asymmetric Zn||Zn cells with a limited mass of plated Zn as the working electrode, the $ZnCl_2$ improves the average CE of the Zn anode to 95.4% from 73.2% in 5 m $ZnCl_2$.

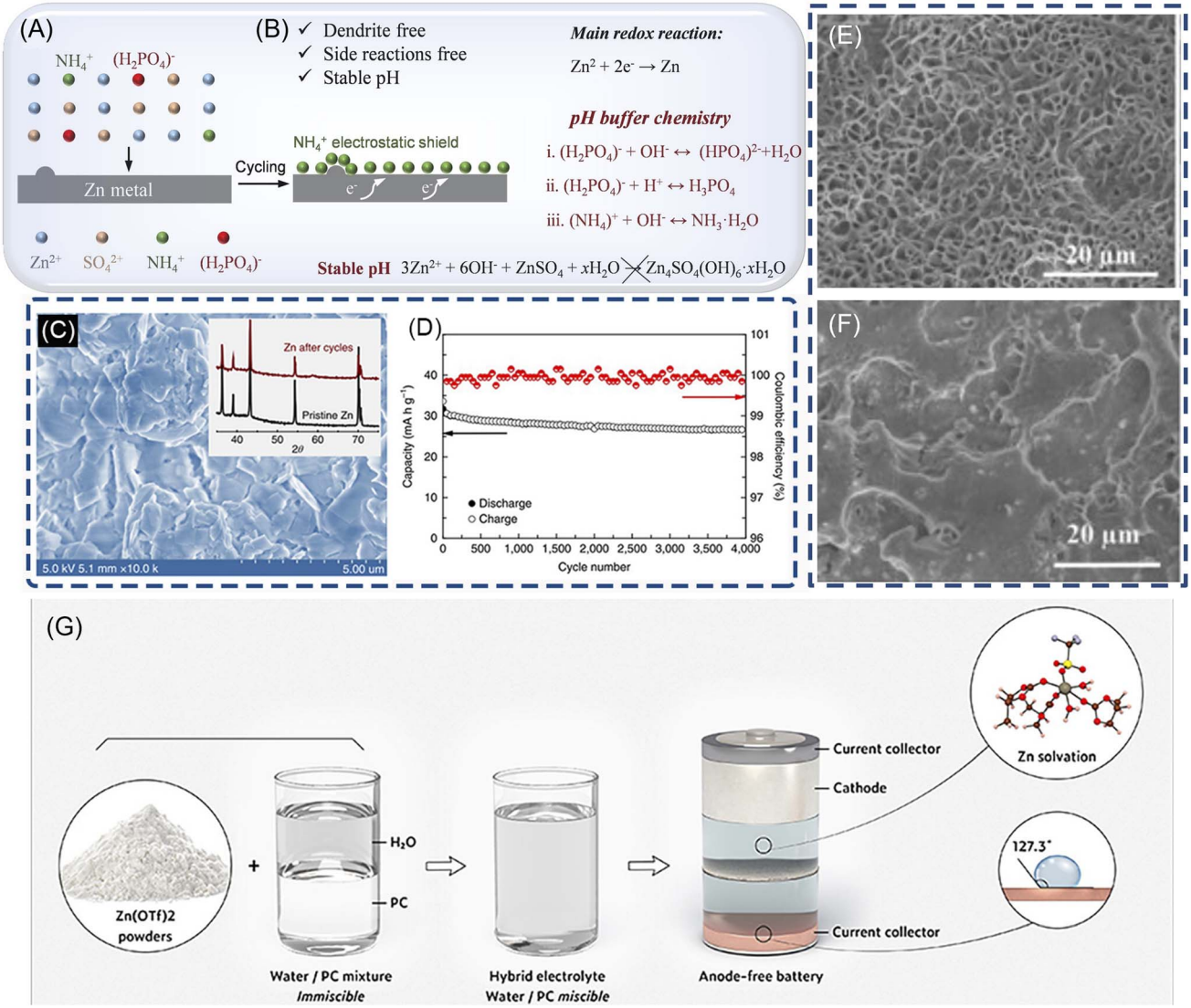

Fig. 7 The schematic diagram of zinc plating processes in (A, B) 1 M $ZnSO_4$ + 25 mM NHP. Reproduced with permission.[106] Copyright 2023, WILEY-VCH. (C). SEM image and XRD pattern (inset) of a Zn anode after 500 stripping/plating cycles in HCZE. (1 M $Zn(TFSI)_2$ + 20 M liTFSI). (D) The cycling stability and CE of the Zn||$LiMn_2O_4$ full cell in HCZE at 4C. Reproduced with permission.[25] Copyright 2018, Springer Nature. (E and F). SEM images of the morphologies grown at the Zn anode after plating/stripping for 1000 times (2000 h) in a 0.5 m $Zn(CF_3SO_3)_2$-TEP electrolyte. Reproduced with permission.[75] Copyright 2019, WILEY-VCH. (G) Schematic illustration of the preparation of the hybrid electrolyte, the corresponding Zn solvation structure, and the resultant hydrophobic interphase. Reproduced with permission.[113] Copyright 2022, American Chemical Society.

However, at a low current density (0.2 mA cm^{-2}) and low plating or stripping capacity (0.03 mA h cm^{-2}), a concentrated electrolyte can cause a relatively large voltage polarization or result in high viscosity and low ionic conductivity, leading to deficient rate performance of Zn anodes.[9,114] Also, the electrolyte with highly concentrate Zn salts is relatively expensive and largely hinders its potential for grid-scale application.

4.4 Organic solvent

Compared to water, organic solvents offer more thermally stable solvation structures with Zn^{2+} ions, a larger ESPW (up to ~3.8 V *vs.* Zn^{2+}/Zn)[115] and are ideal electrolytes for ZIBs that can suppress dendrite formation and minimize side reactions.[101,116–118] Triethyl phosphate (TEP) was introduced as a cosolvent and solvent with aqueous electrolytes to stabilize the Zn electrode and enhance CE.[75] In TEP solution, $Zn_3(PO_4)_2$ forms on the anode surface, serving as an *in situ* formed molecular template to guide Zn nucleation and produce porous morphology instead of dendrites (Fig. 7E and F). Full Zn||potassium copper hexacyanoferrate (KCuHCf) cells with this electrolyte exhibit good cycling stability with an average CE of 97.66% after 1000 cycles (electrolyte: 0.5 m $Zn(CF_3SO_3)_2$–TEP–H_2O). Appropriate control of water content is necessary since excess water negatively affects cycling performance (Fig. 7G). This research offers insights for developing safer organic electrolytes. In another study, a salting-in-effect-

induced hybrid electrolyte is proposed as an effective strategy that enables both a highly reversible Zn anode and good stability and compatibility toward various cathodes.[113] The as-prepared electrolyte can also work well under a wide temperature range (*i.e.*, from −20 to 50 °C). It is demonstrated that in the presence of propylene carbonate, triflate anions are involved in the Zn^{2+} solvation sheath structure, even at a low salt concentration (2.14 M). The unique solvation structure results in the reduction of anions, thus forming a hydrophobic solid electrolyte interphase. The waterproof interphase along with the decreased water activity in the hybrid electrolyte effectively prevents side reactions, thus ensuring a stable Zn anode with an unprecedented CE (99.93% over 500 cycles at 1 mA cm^{-2}). The author design an anode-free Zn metal battery that exhibits excellent cycling stability (80% capacity retention after 275 cycles at 0.5 mA cm^{-2}) (electrolyte: *X*% ((30%, 50%, 70%, 90%) PC-$Zn(OTf)_2$).

5. Analytical technology

Apart from the above strategies focusing on materials, analytical technology is also a necessary tool to figure out the specific reactions inside batteries during charge/discharge processes. Various characterization techniques can provide comprehensive analysis of the Zn anode, including electronic structure analysis, chemical composition analysis, morphological structure analysis, crystallinity analysis, and electrochemical evaluation. Furthermore, simulations and calculations can be conducted to offer reasonable predictions and atomic-level explanations concerning the failure mechanism of the Zn anode and the effectiveness of protection strategies (Fig. 8).

The conventional characterizations of Zn anode include scanning electron microscope (SEM), Atomic force microscopy (AFM), X-ray diffraction (XRD), X-ray photoelectron spectroscopy (XPS), Raman and Fourier-transform infrared spectroscopy (FTIR) *etc.* For instance, the formation and dissolution of Zn dendrite in a cell can be clearly shown by SEM.[119] It was established that the dendrites start to form on surface inhomogeneities where the local current is high, and proceed to grow to a final state with various length dendrites present on the electrode surface, with the longest dendrites having the shortest initiation time. Moreover, the higher the operational current density, the shorter and bigger were the initiation time and the dendrite height, respectively. AFM can be further employed to investigate the mechanism of dendritic nucleation and growth because it could characterize the surface morphology and roughness information well.[120] The issues mentioned above, namely dendrite formation, chemical corrosion, hydrogen evolution, and slow kinetics, can be clearly observed in the electrochemical data of Zn anodes. Electrochemical characterizations are capable of directly revealing the electrochemical properties of the materials and determining the effectiveness of strategies used to address these issues. Several typical electrochemical characterization methods commonly used to study Zn anodes include galvanostatic cycling test, CE, depth of discharge (DOD), linear sweep voltammetry (LSV), electrochemical impedance spectroscopy (EIS).[39,121]

In situ characterization techniques are crucial research methods in electrochemical reaction processes. They enable real-time detection of changes in chemical composition, morphological structure, surface condition, crystallinity, valence state, and other relevant factors during reaction processes. This capability is of great significance for exploring the underlying mechanisms in greater depth and developing practical applications. Smith *et al.* conducted an *in situ* investigation using AFM synchronized with a quartz crystal

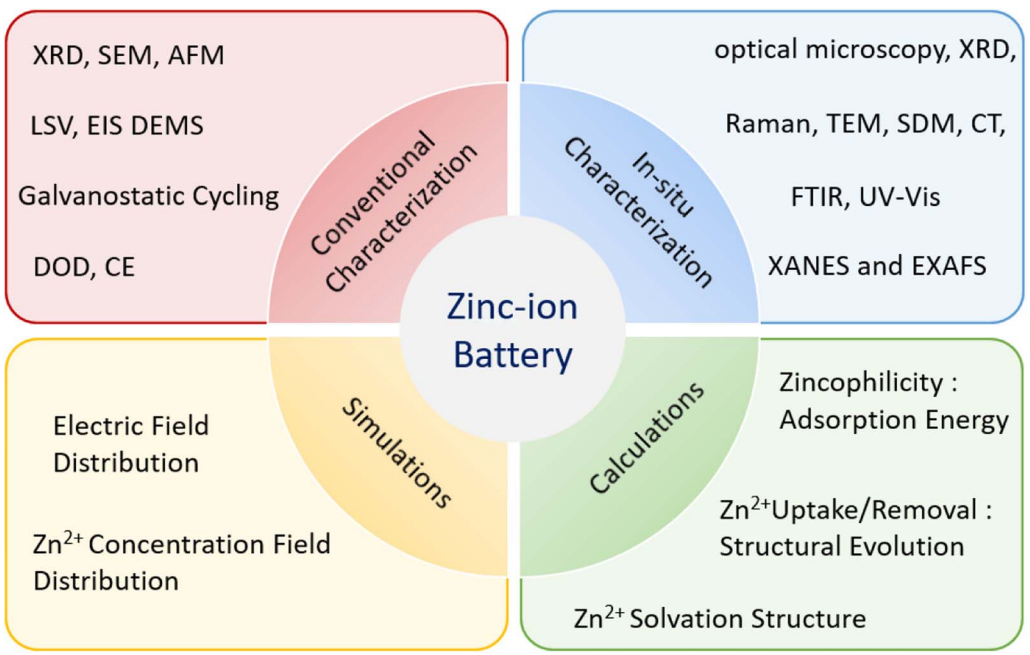

Fig. 8 The reported interface characterization techniques and analysis methods.

microbalance (QCM) to resolve both nucleation and growth of zinc on gold during electrodeposition with choline chloride based deep eutectic solvents.[122] Other advanced characterization methods, such as neutron scattering and synchrotron X-radiation (SXR), X-ray absorption spectroscopy (XAS) have also been applied to this field. However, post-mortem studies on the SEI may be impacted by operational or environmental factors, which can limit their ability to fully capture the ongoing processes. Therefore, the development of *in situ* spectroscopic measurements is critical for revealing the surface chemistry of actual Zn anodes.[76,123–125]

6. Summary and perspective

ZIBs have been regarded as competitive alternatives of LIBs in large-scale energy storage system, and a summary of solutions for the protection of Zn metal anode in the aqueous electrolyte is shown in Fig. 9.

6.1 Zn anode

In response to the current problems with Zn anodes, researchers have proposed several effective solutions, including surface coating, and changing the structure of the anode. However, Zn anode need to be modified by "*ex situ*" methods mentioned above and then used in the battery. More research needs to be focused on simple methods that can generate a protective layer by the "*in situ*" process. Meanwhile, the inherent mechanism of controllable Zn deposition is still unclear. *In situ* characterization of Zn plating/stripping processes can capture the initial states of dendrite formation, distribution of nucleation sites, and migration of Zn ions on the surface, which are quite essential in designing the Zn anodes with high stability, for instance, *in situ* XRD, Raman, FTIR, and AFM, *etc.* However, these technique always need large current density, the increasing current density will raise the local charge density and thus intensify voltage hysteresis, resulting in uneven Zn deposition, easily induces dendrite formation. As for the Zn foil surface coating, new research methods to accurately control the thickness of the film layer, the amount of the coating layer, are worth being developed. In addition, the utilization rate of Zn anodes seems to be overlooked. In the current research, Zn foils are always simply used as the Zn anodes. In fact, the actual consumed amount of Zn anode in a cell is also a major research direction to reduce the cost and improve the battery performance.

6.2 Electrolyte

The most important principle is to ensure its stable existence with the electrode. At the same time, it is necessary to keep high ionic conductivity, a wide working voltage window, and environmental friendliness. In the design of aqueous electrolytes, high-concentration electrolytes have solved dendrites and corrosion problems of Zn anodes, but with the increase of the electrolyte concentration, the cost of whole batteries will be increased. Therefore, electrolyte additives seem to be a more economical way for large-scale energy storage systems. During the cycling process of the ZIB, the change of pH due to the HER especially near the electrode surface is a problem worthy of attention and study. During different states of the charge and discharge processes, the pH changes continuously, which seriously affects its cycling stability. Adding a suitable pH buffer into the electrolyte may alleviate this problem. At the same time, the influence from different electrolyte additives on cathode materials need to be fully considered. Besides the typical Zn^{2+} intercalation chemistry,[126–128] other reaction mechanisms such as co-insertion of cations (H^+, Li^+, Na^+),[129–131] structural water in cathode crystals[132–134] play crucial roles to guide the design of novel and high-performance ZIBs. The unknown interfacial phenomena need to be unfolded by advanced characterization techniques to comprehensive understanding of Zn anode/

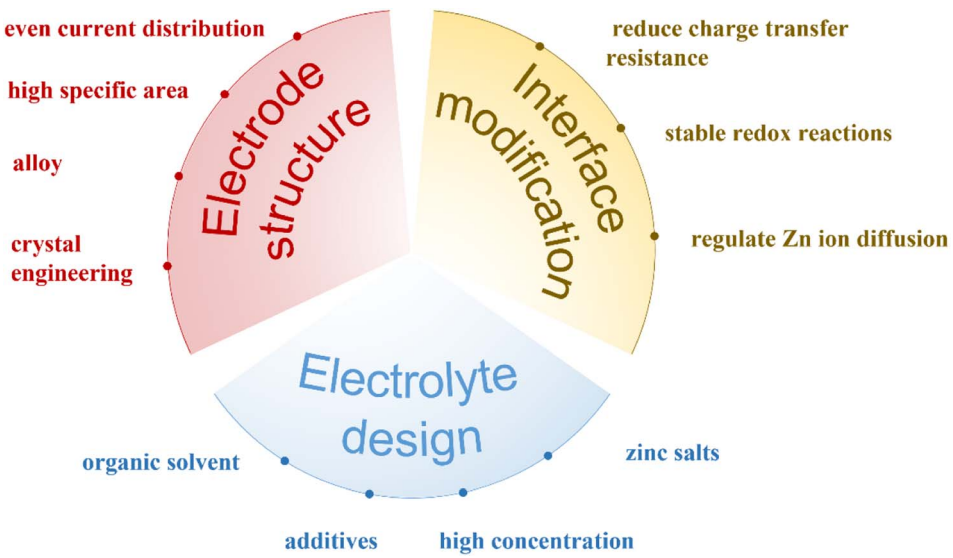

Fig. 9 Summary and categories of the existing strategies towards dendrite-free Zn anodes.

electrolyte interfaces. *In situ* characterization techniques are highly desired to pursue the real-time interface evolution.

6.3 Cathode

The cathode material has several serious issues, including active material dissolution, structural collapse, fast capacity decay, low capacity, low operating voltage, and sluggish reaction kinetics. The functional limitations of the cathode are another main reason why aqueous ZIBs cannot be practically used. Adding additives to the electrolyte can efficiently protect the cathode, improve cycle stability, and increase capacity and operating voltage, among other benefits. However, there are still many questions to be solved. For example, with using the additive, many of the reaction mechanisms are still unclear; there is no report about the additive broad applicability for different cathode materials.

On the other hand, the separator is another important component in batteries to prevent short circuiting; more than 98% of studies on ZIBs use glass fibers or filter papers. A few studies have used a polymer-based separator such as Celgard[135,136] or Nafion membrane.[137] To date, there is a lack of systematic studies of separator materials in ZIBs. It is easy to understand the good compatibility of glass fibers in an aqueous electrolyte; however, the glass fibers are fragile, expensive and not as flexible as polymer-based separators. While the effect of separator compositions on battery performance may not be as critical as electrolytes, researchers must address this issue for the successful commercialization of ZIBs.

Conflicts of interest

There are no conflicts to declare.

Acknowledgements

The authors would like to acknowledge Engineering and Physical Sciences Research Council (EP/V027433/2) and UK Research and Innovation (UKRI) under the UK government's Horizon Europe funding guarantee (101077226; EP/Y008707/1) for funding support.

References

1 J. B. Goodenough and Y. Kim, *Chem. Mater.*, 2010, **22**, 587–603.
2 Y. Zhang, Y. Zhong, Z. Wu, B. Wang, S. Liang and H. Wang, *Angew. Chem., Int. Ed.*, 2020, **59**, 7797–7802.
3 H. Zhang, H. Zhao, M. A. Khan, W. Zou, J. Xu, L. Zhang and J. Zhang, *J. Mater. Chem. A*, 2018, **6**, 20564–20620.
4 K. Xu, *Chem. Rev.*, 2014, **114**, 11503–11618.
5 D. Lin, Y. Liu and Y. Cui, *Nat. Nanotechnol.*, 2017, **12**, 194.
6 N. Zhang, X. Chen, M. Yu, Z. Niu, F. Cheng and J. Chen, *Chem. Soc. Rev.*, 2020, **49**, 4203–4219.
7 D. Kundu, B. D. Adams, V. Duffort, S. H. Vajargah and L. F. Nazar, *Nat. Energy*, 2016, **1**, 16119.
8 B. Tang, L. Shan, S. Liang and J. Zhou, *Energy Environ. Sci.*, 2019, **12**, 3288–3304.
9 L. E. Blanc, D. Kundu and L. F. Nazar, *Joule*, 2020, **4**, 771–799.
10 A. Ponrouch, C. Frontera, F. Bardé and M. R. Palacín, *Nat. Mater.*, 2016, **15**, 169–172.
11 H. D. Yoo, I. Shterenberg, Y. Gofer, G. Gershinsky, N. Pour and D. Aurbach, *Energy Environ. Sci.*, 2013, **6**, 2265–2279.
12 J. Muldoon, C. B. Bucur, A. G. Oliver, T. Sugimoto, M. Matsui, H. S. Kim, G. D. Allred, J. Zajicek and Y. Kotani, *Energy Environ. Sci.*, 2012, **5**, 5941–5950.
13 E. Levi, Y. Gofer and D. Aurbach, *Chem. Mater.*, 2010, **22**, 860–868.
14 Y. NuLi, J. Yang, Y. Li and J. Wang, *Chem. Commun.*, 2010, **46**, 3794–3796.
15 S. K. Das, S. Mahapatra and H. Lahan, *J. Mater. Chem. A*, 2017, **5**, 6347–6367.
16 G. A. Elia, K. Marquardt, K. Hoeppner, S. Fantini, R. Lin, E. Knipping, W. Peters, J. F. Drillet, S. Passerini and R. Hahn, *Adv. Mater.*, 2016, **28**, 7564–7579.
17 S. Liu, J. Hu, N. Yan, G. Pan, G. Li and X. Gao, *Energy Environ. Sci.*, 2012, **5**, 9743–9746.
18 H. Pan, Y. Shao, P. Yan, Y. Cheng, K. S. Han, Z. Nie, C. Wang, J. Yang, X. Li, P. Bhattacharya, K. T. Mueller and J. Liu, *Nat. Energy*, 2016, **1**, 7.
19 N. Zhang, F. Y. Cheng, J. X. Liu, L. B. Wang, X. H. Long, X. S. Liu, F. J. Li and J. Chen, *Nat. Commun.*, 2017, **8**, 9.
20 J. Ming, J. Guo, C. Xia, W. Wang and H. N. Alshareef, *Mater. Sci. Eng., R*, 2019, **135**, 58–84.
21 D. Chao, W. Zhou, C. Ye, Q. Zhang, Y. Chen, L. Gu, K. Davey and S.-Z. Qiao, *Angew. Chem., Int. Ed.*, 2019, **58**, 7823–7828.
22 G. He, X. Han, R. Zou, T. Zhao, Z. Weng, S. Ho-Kimura, Y. Lu, H. Wang, Z. X. Guo and I. P. Parkin, *Adv. Funct. Mater.*, 2017, **27**, 1604903.
23 Y. Liu, X. Lu, F. Lai, T. Liu, P. R. Shearing, I. P. Parkin, G. He and D. J. L. Brett, *Joule*, 2021, **5**, 2845–2903.
24 T. B. Reddy, *Linden's handbook of batteries*, Mcgraw-hill, New York, vol. 4, 2011.
25 F. Wang, O. Borodin, T. Gao, X. Fan, W. Sun, F. Han, A. Faraone, J. A. Dura, K. Xu and C. Wang, *Nat. Mater.*, 2018, **17**, 543–549.
26 N. Zhang, F. Y. Cheng, Y. C. Liu, Q. Zhao, K. X. Lei, C. C. Chen, X. S. Liu and J. Chen, *J. Am. Chem. Soc.*, 2016, **138**, 12894–12901.
27 C. Xia, J. Guo, Y. Lei, H. Liang, C. Zhao and H. N. Alshareef, *Adv. Mater.*, 2018, **30**, 1705580.
28 C. Xia, J. Guo, P. Li, X. Zhang and H. N. Alshareef, *Angew. Chem., Int. Ed.*, 2018, **57**, 3943–3948.
29 W. Kao-ian, R. Pornprasertsuk, P. Thamyongkit, T. Maiyalagan and S. Kheawhom, *J. Electrochem. Soc.*, 2019, **166**, A1063–A1069.
30 C. Zhang, J. Holoubek, X. Wu, A. Daniyar, L. Zhu, C. Chen, D. P. Leonard, I. A. Rodríguez-Pérez, J.-X. Jiang, C. Fang and X. Ji, *Chem. Commun.*, 2018, **54**, 14097–14099.
31 J. Zheng, Q. Zhao, T. Tang, J. Yin, C. D. Quilty, G. D. Renderos, X. Liu, Y. Deng, L. Wang, D. C. Bock, C. Jaye, D. Zhang, E. S. Takeuchi, K. J. Takeuchi,

A. C. Marschilok and L. A. Archer, *Science*, 2019, **366**, 645–648.
32 R. Parsons, *Surf. Sci.*, 1964, **2**, 418–435.
33 A. Konarov, N. Voronina, J. H. Jo, Z. Bakenov, Y.-K. Sun and S.-T. Myung, *ACS Energy Lett.*, 2018, **3**, 2620–2640.
34 M. Song, H. Tan, D. Chao and H. J. Fan, *Adv. Funct. Mater.*, 2018, **28**, 1802564.
35 M. C. H. McKubre, *J. Electrochem. Soc.*, 1981, **128**, 524.
36 P. Gu, M. Zheng, Q. Zhao, X. Xiao, H. Xue and H. Pang, *J. Mater. Chem. A*, 2017, **5**, 7651–7666.
37 C. Han, W. Li, H. K. Liu, S. Dou and J. Wang, *Nano Energy*, 2020, **74**, 104880.
38 W. Sun, F. Wang, S. Hou, C. Yang, X. Fan, Z. Ma, T. Gao, F. Han, R. Hu and M. Zhu, *J. Am. Chem. Soc.*, 2017, **139**, 9775–9778.
39 Z. Zhao, J. Zhao, Z. Hu, J. Li, J. Li, Y. Zhang, C. Wang and G. Cui, *Energy Environ. Sci.*, 2019, **12**, 1938–1949.
40 J. Hao, X. Li, S. Zhang, F. Yang, X. Zeng, S. Zhang, G. Bo, C. Wang and Z. Guo, *Adv. Funct. Mater.*, 2020, **30**, 2001263.
41 H. He, H. Tong, X. Song, X. Song and J. Liu, *J. Mater. Chem. A*, 2020, **8**, 7836–7846.
42 S.-B. Wang, Q. Ran, R.-Q. Yao, H. Shi, Z. Wen, M. Zhao, X.-Y. Lang and Q. Jiang, *Nat. Commun.*, 2020, **11**, 1634.
43 Y. Yan, Y. Zhang, Y. Wu, Z. Wang, A. Mathur, H. Yang, P. Chen, S. Nair and N. Liu, *ACS Appl. Energy Mater.*, 2018, **1**, 6345–6351.
44 L. Dai, T. Wang, B. Jin, N. Liu, Y. Niu, W. Meng, Z. Gao, X. Wu, L. Wang and Z. He, *Surf. Coat. Technol.*, 2021, **427**, 127813.
45 B. Li, J. Xue, C. Han, N. Liu, K. Ma, R. Zhang, X. Wu, L. Dai, L. Wang and Z. He, *J. Colloid Interface Sci.*, 2021, **599**, 467–475.
46 M. Zhou, S. Guo, G. Fang, H. Sun, X. Cao, J. Zhou, A. Pan and S. Liang, *J. Energy Chem.*, 2021, **55**, 549–556.
47 B. Li, J. Xue, X. Lv, R. Zhang, K. Ma, X. Wu, L. Dai, L. Wang and Z. He, *Surf. Coat. Technol.*, 2021, **421**, 127367.
48 P. Liang, J. Yi, X. Liu, K. Wu, Z. Wang, J. Cui, Y. Liu, Y. Wang, Y. Xia and J. Zhang, *Adv. Funct. Mater.*, 2020, **30**, 1908528.
49 S. Bhoyate, S. Mhin, J.-e. Jeon, K. Park, J. Kim and W. Choi, *ACS Appl. Mater. Interfaces*, 2020, **12**, 27249–27257.
50 X. Xie, S. Liang, J. Gao, S. Guo, J. Guo, C. Wang, G. Xu, X. Wu, G. Chen and J. Zhou, *Energy Environ. Sci.*, 2020, **13**, 503–510.
51 H. Liu, J.-G. Wang, W. Hua, H. Sun, Y. Huyan, S. Tian, Z. Hou, J. Yang, C. Wei and F. Kang, *Adv. Sci.*, 2021, **8**, 2102612.
52 Y. Huyan, J.-G. Wang, S. Tian, L. Ren, H. Liu and B. Wei, *EcoMat*, 2022, **4**, e12173.
53 Z. Wang, J. Huang, Z. Guo, X. Dong, Y. Liu, Y. Wang and Y. Xia, *Joule*, 2019, **3**, 1289–1300.
54 W. Li, K. Wang, M. Zhou, H. Zhan, S. Cheng and K. Jiang, *ACS Appl. Mater. Interfaces*, 2018, **10**, 22059–22066.
55 Y. Du, C. Liu, Y. Liu, Q. Han, X. Chi and Y. Liu, *Electrochim. Acta*, 2020, **339**, 135867.
56 Z. Zhou, Y. Zhang, P. Chen, Y. Wu, H. Yang, H. Ding, Y. Zhang, Z. Wang, X. Du and N. Liu, *Chem. Eng. Sci.*, 2019, **194**, 142–147.
57 A. Wang, W. Zhou, A. Huang, M. Chen, J. Chen, Q. Tian and J. Xu, *J. Colloid Interface Sci.*, 2020, **577**, 256–264.
58 M. Qiu, D. Wang, B. Tawiah, H. Jia, B. Fei and S. Fu, *Composites, Part B*, 2021, **215**, 108798.
59 A. Xia, X. Pu, Y. Tao, H. Liu and Y. Wang, *Appl. Surf. Sci.*, 2019, **481**, 852–859.
60 C. Shen, X. Li, N. Li, K. Xie, J.-g. Wang, X. Liu and B. Wei, *ACS Appl. Mater. Interfaces*, 2018, **10**, 25446–25453.
61 L. Dong, W. Yang, W. Yang, H. Tian, Y. Huang, X. Wang, C. Xu, C. Wang, F. Kang and G. Wang, *Chem. Eng. J.*, 2020, **384**, 123355.
62 L. Kang, M. Cui, F. Jiang, Y. Gao, H. Luo, J. Liu, W. Liang and C. Zhi, *Adv. Energy Mater.*, 2018, **8**, 1801090.
63 B. Li, B. Jin, R. Zhang, K. Ma, X. Wu, L. Dai, L. Wang and Z. He, *Surf. Coat. Technol.*, 2021, **425**, 127699.
64 T. Wang, Q. Xi, Y. Li, H. Fu, Y. Hua, E. G. Shankar, A. K. Kakarla and J. S. Yu, *Adv. Sci.*, 2022, **9**, e2200155.
65 Y. Xia, H. Wang, G. Shao and C.-A. Wang, *J. Power Sources*, 2022, **540**, 231659.
66 P. Chen, X. Yuan, Y. Xia, Y. Zhang, L. Fu, L. Liu, N. Yu, Q. Huang, B. Wang, X. Hu, Y. Wu and T. van Ree, *Adv. Sci.*, 2021, **8**, e2100309.
67 Z. Cao, X. Zhu, D. Xu, P. Dong, M. O. L. Chee, X. Li, K. Zhu, M. Ye and J. Shen, *Energy Stor. Mater.*, 2021, **36**, 132–138.
68 Q. Jian, Y. Wan, Y. Lin, M. Ni, M. Wu and T. Zhao, *ACS Appl. Mater. Interfaces*, 2021, **13**, 52659–52669.
69 J. Hao, X. Li, S. Zhang, F. Yang, X. Zeng, S. Zhang, G. Bo, C. Wang and Z. Guo, *Adv. Funct. Mater.*, 2020, **30**, 2001263.
70 M. Zhu, J. Hu, Q. Lu, H. Dong, D. D. Karnaushenko, C. Becker, D. Karnaushenko, Y. Li, H. Tang, Z. Qu, J. Ge and O. G. Schmidt, *Adv. Mater.*, 2021, **33**, 2007497.
71 L. Zhang, J. Huang, H. Guo, L. Ge, Z. Tian, M. Zhang, J. Wang, G. He, T. Liu, J. Hofkens, D. J. L. Brett and F. Lai, *Adv. Energy Mater.*, 2023, **13**, 2203790.
72 M. Cui, Y. Xiao, L. Kang, W. Du, Y. Gao, X. Sun, Y. Zhou, X. Li, H. Li and F. Jiang, *ACS Appl. Energy Mater.*, 2019, **2**, 6490–6496.
73 H. Yang, Z. Chang, Y. Qiao, H. Deng, X. Mu, P. He and H. Zhou, *Angew. Chem., Int. Ed.*, 2020, **59**, 9377–9381.
74 Z. Cai, Y. Ou, J. Wang, R. Xiao, L. Fu, Z. Yuan, R. Zhan and Y. Sun, *Energy Stor. Mater.*, 2020, **27**, 205–211.
75 A. Naveed, H. Yang, J. Yang, Y. Nuli and J. Wang, *Angew. Chem., Int. Ed.*, 2019, **58**, 2760–2764.
76 D. Han, S. Wu, S. Zhang, Y. Deng, C. Cui, L. Zhang, Y. Long, H. Li, Y. Tao and Z. Weng, *Small*, 2020, **16**, 2001736.
77 K. Hu, X. Guan, R. Lv, G. Li, Z. Hu, L. Ren, A. Wang, X. Liu and J. Luo, *Chem. Eng. J.*, 2020, **396**, 125363.
78 W. Guo, Y. Zhang, X. Tong, X. Wang, L. Zhang, X. Xia and J. Tu, *Mater. Today Energy*, 2021, **20**, 100675.
79 Y. Wang, Y. Chen, W. Liu, X. Ni, P. Qing, Q. Zhao, W. Wei, X. Ji, J. Ma and L. Chen, *J. Mater. Chem. A*, 2021, **9**, 8452–8461.

80 K. Zhao, C. Wang, Y. Yu, M. Yan, Q. Wei, P. He, Y. Dong, Z. Zhang, X. Wang and L. Mai, *Adv. Mater. Interfaces*, 2018, **5**, 1800848.
81 J. Zhou, M. Xie, F. Wu, Y. Mei, Y. Hao, R. Huang, G. Wei, A. Liu, L. Li and R. Chen, *Adv. Mater.*, 2021, **33**, 2101649.
82 M. Li, Q. He, Z. Li, Q. Li, Y. Zhang, J. Meng, X. Liu, S. Li, B. Wu, L. Chen, Z. Liu, W. Luo, C. Han and L. Mai, *Adv. Energy Mater.*, 2019, **9**, 1901469.
83 H. Liu, Q. Ye, D. Lei, Z. Hou, W. Hua, Y. Huyan, N. Li, C. Wei, F. Kang and J.-G. Wang, *Energy Environ. Sci.*, 2023, **16**, 1610–1619.
84 H. Liu, J.-G. Wang, W. Hua, L. Ren, H. Sun, Z. Hou, Y. Huyan, Y. Cao, C. Wei and F. Kang, *Energy Environ. Sci.*, 2022, **15**, 1872–1881.
85 H. Li, Z. Liu, G. Liang, Y. Huang, Y. Huang, M. Zhu, Z. Pei, Q. Xue, Z. Tang and Y. Wang, *ACS Nano*, 2018, **12**, 3140–3148.
86 G. Garcia, E. Ventosa and W. Schuhmann, *ACS Appl. Mater. Interfaces*, 2017, **9**, 18691–18698.
87 Y. Zeng, X. Zhang, Y. Meng, M. Yu, J. Yi, Y. Wu, X. Lu and Y. Tong, *Adv. Mater.*, 2017, **29**, 1700274.
88 L.-P. Wang, N.-W. Li, T.-S. Wang, Y.-X. Yin, Y.-G. Guo and C.-R. Wang, *Electrochim. Acta*, 2017, **244**, 172–177.
89 Y. Zeng, X. Zhang, R. Qin, X. Liu, P. Fang, D. Zheng, Y. Tong and X. Lu, *Adv. Mater.*, 2019, **31**, 1903675.
90 Q. Zhang, J. Luan, L. Fu, S. Wu, Y. Tang, X. Ji and H. Wang, *Angew. Chem., Int. Ed.*, 2019, **58**, 15841–15847.
91 C. Li, X. Shi, S. Liang, X. Ma, M. Han, X. Wu and J. Zhou, *Chem. Eng. J.*, 2020, **379**, 122248.
92 Z. Kang, C. Wu, L. Dong, W. Liu, J. Mou, J. Zhang, Z. Chang, B. Jiang, G. Wang, F. Kang and C. Xu, *ACS Sustainable Chem. Eng.*, 2019, **7**, 3364–3371.
93 M. A. González, R. Trócoli, I. Pavlovic, C. Barriga and F. La Mantia, *Electrochem. Commun.*, 2016, **68**, 1–4.
94 D. Wang, L. Wang, G. Liang, H. Li, Z. Liu, Z. Tang, J. Liang and C. Zhi, *ACS Nano*, 2019, **13**, 10643–10652.
95 N. V. Narayanan, B. Ashokraj and S. Sampath, *J. Colloid Interface Sci.*, 2010, **342**, 505–512.
96 G. Kasiri, R. Trócoli, A. Bani Hashemi and F. La Mantia, *Electrochim. Acta*, 2016, **222**, 74–83.
97 N. Zhang, F. Cheng, Y. Liu, Q. Zhao, K. Lei, C. Chen, X. Liu and J. Chen, *J. Am. Chem. Soc.*, 2016, **138**, 12894–12901.
98 J. Huang, Z. Guo, Y. Ma, D. Bin, Y. Wang and Y. Xia, *Small Methods*, 2019, **3**, 1800272.
99 B. Lee, H. R. Seo, H. R. Lee, C. S. Yoon, J. H. Kim, K. Y. Chung, B. W. Cho and S. H. Oh, *ChemSusChem*, 2016, **9**, 2948–2956.
100 X. Zeng, J. Hao, Z. Wang, J. Mao and Z. Guo, *Energy Stor. Mater.*, 2019, **20**, 410–437.
101 D. Han, C. Cui, K. Zhang, Z. Wang, J. Gao, Y. Guo, Z. Zhang, S. Wu, L. Yin, Z. Weng, F. Kang and Q.-H. Yang, *Nat. Sustain.*, 2022, **5**, 205–213.
102 N. Zhang, F. Cheng, Y. Liu, Q. Zhao, K. Lei, C. Chen, X. Liu and J. Chen, *J. Am. Chem. Soc.*, 2016, **138**, 12894–12901.
103 F. Wan, L. Zhang, X. Dai, X. Wang, Z. Niu and J. Chen, *Nat. Commun.*, 2018, **9**, 1656.
104 K. E. K. Sun, T. K. A. Hoang, T. N. L. Doan, Y. Yu, X. Zhu, Y. Tian and P. Chen, *ACS Appl. Mater. Interfaces*, 2017, **9**, 9681–9687.
105 H. Dong, R. Liu, X. Hu, F. Zhao, L. Kang, L. Liu, J. Li, Y. Tan, Y. Zhou, D. J. L. Brett, G. He and I. P. Parkin, *Adv. Sci.*, 2023, **10**, 2205084.
106 W. Zhang, Y. Dai, R. Chen, Z. Xu, J. Li, W. Zong, H. Li, Z. Li, Z. Zhang, J. Zhu, F. Guo, X. Gao, Z. Du, J. Chen, T. Wang, G. He and I. P. Parkin, *Angew. Chem., Int. Ed.*, 2023, **62**, e202212695.
107 X. Gao, Y. Dai, C. Zhang, Y. Zhang, W. Zong, W. Zhang, R. Chen, J. Zhu, X. Hu, M. Wang, R. Chen, Z. Du, F. Guo, H. Dong, Y. Liu, H. He, S. Zhao, F. Zhao, J. Li, I. P. Parkin, C. J. Carmalt and G. He, *Angew. Chem., Int. Ed.*, 2023, **135**, e202300608.
108 R. Chen, C. Zhang, J. Li, Z. Du, F. Guo, W. Zhang, Y. Dai, W. Zong, X. Gao, J. Zhu, Y. Zhao, X. Wang and G. He, *Energy Environ. Sci.*, 2023, DOI: **10.1039/d3ee00462g**.
109 X. Guo, Z. Zhang, J. Li, N. Luo, G.-L. Chai, T. S. Miller, F. Lai, P. Shearing, D. J. L. Brett, D. Han, Z. Weng, G. He and I. P. Parkin, *ACS Energy Lett.*, 2021, **6**, 395–403.
110 D. Han, Z. Wang, H. Lu, H. Li, C. Cui, Z. Zhang, R. Sun, C. Geng, Q. Liang, X. Guo, Y. Mo, X. Zhi, F. Kang, Z. Weng and Q.-H. Yang, *Adv. Energy Mater.*, 2022, 2102982.
111 F. Zhao, Z. Jing, X. Guo, J. Li, H. Dong, Y. Tan, L. Liu, Y. Zhou, R. Owen, P. R. Shearing, D. J. L. Brett, G. He and I. P. Parkin, *Energy Stor. Mater.*, 2022, **53**, 638–645.
112 Y. Jin, K. S. Han, Y. Shao, M. L. Sushko, J. Xiao, H. Pan and J. Liu, *Adv. Funct. Mater.*, 2020, **30**, 2003932.
113 F. Ming, Y. Zhu, G. Huang, A. H. Emwas, H. Liang, Y. Cui and H. N. Alshareef, *J. Am. Chem. Soc.*, 2022, **144**(16), 7160–7170.
114 Z. Ye, Z. Cao, M. O. Lam Chee, P. Dong, P. M. Ajayan, J. Shen and M. Ye, *Energy Stor. Mater.*, 2020, **32**, 290–305.
115 S.-D. Han, N. N. Rajput, X. Qu, B. Pan, M. He, M. S. Ferrandon, C. Liao, K. A. Persson and A. K. Burrell, *ACS Appl. Mater. Interfaces*, 2016, **8**, 3021–3031.
116 M. S. Chae, J. W. Heo, H. H. Kwak, H. Lee and S.-T. Hong, *J. Power Sources*, 2017, **337**, 204–211.
117 D. Kundu, S. H. Vajargah, L. Wan, B. Adams, D. Prendergast and L. F. Nazar, *Energy Environ. Sci.*, 2018, **11**, 881–892.
118 F. Wang, W. Sun, Z. Shadike, E. Hu, X. Ji, T. Gao, X.-Q. Yang, K. Xu and C. Wang, *Angew. Chem., Int. Ed.*, 2018, **57**, 11978–11981.
119 V. Yufit, F. Tariq, D. S. Eastwood, M. Biton, B. Wu, P. D. Lee and N. P. Brandon, *Joule*, 2019, **3**, 485–502.
120 Q. Yang, G. Liang, Y. Guo, Z. Liu, B. Yan, D. Wang, Z. Huang, X. Li, J. Fan and C. Zhi, *Adv. Mater.*, 2019, **31**, 1903778.
121 Y. Dong, L. Miao, G. Ma, S. Di, Y. Wang, L. Wang, J. Xu and N. Zhang, *Chem. Sci.*, 2021, **12**, 5843–5852.
122 E. L. Smith, J. C. Barron, A. P. Abbott and K. S. Ryder, *Anal. Chem.*, 2009, **81**, 8466–8471.
123 Y. Sasaki, K. Yoshida, T. Kawasaki, A. Kuwabara, Y. Ukyo and Y. Ikuhara, *J. Power Sources*, 2021, **481**, 228831.

124 A. Nakata, H. Murayama, K. Fukuda, T. Yamane, H. Arai, T. Hirai, Y. Uchimoto, J.-i. Yamaki and Z. Ogumi, *Electrochim. Acta*, 2015, **166**, 82–87.
125 J. Dogel and W. Freyland, *Phys. Chem. Chem. Phys.*, 2003, **5**, 2484–2487.
126 L. Zhang, L. Chen, X. Zhou and Z. Liu, *Adv. Energy Mater.*, 2015, **5**, 1400930.
127 M. H. Alfaruqi, J. Gim, S. Kim, J. Song, D. T. Pham, J. Jo, Z. Xiu, V. Mathew and J. Kim, *Electrochem. Commun.*, 2015, **60**, 121–125.
128 X. Dai, F. Wan, L. Zhang, H. Cao and Z. Niu, *Energy Stor. Mater.*, 2019, **17**, 143–150.
129 S. Islam, M. H. Alfaruqi, D. Y. Putro, V. Soundharrajan, B. Sambandam, J. Jo, S. Park, S. Lee, V. Mathew and J. Kim, *J. Mater. Chem. A*, 2019, **7**, 20335–20347.
130 Y. Yang, Y. Tang, G. Fang, L. Shan, J. Guo, W. Zhang, C. Wang, L. Wang, J. Zhou and S. Liang, *Energy Environ. Sci.*, 2018, **11**, 3157–3162.
131 K. Zhu, T. Wu and K. Huang, *ACS Nano*, 2019, **13**, 14447–14458.
132 J. Shin, D. S. Choi, H. J. Lee, Y. Jung and J. W. Choi, *Adv. Energy Mater.*, 2019, **9**, 1900083.
133 M. Yan, P. He, Y. Chen, S. Wang, Q. Wei, K. Zhao, X. Xu, Q. An, Y. Shuang, Y. Shao, K. T. Mueller, L. Mai, J. Liu and J. Yang, *Adv. Mater.*, 2018, **30**, 1703725.
134 K. Zhu, T. Wu and K. Huang, *Adv. Energy Mater.*, 2019, **9**, 1901968.
135 C. Pan, R. Zhang, R. G. Nuzzo and A. A. Gewirth, *Adv. Energy Mater.*, 2018, **8**, 1800589.
136 C. Pan, R. G. Nuzzo and A. A. Gewirth, *Chem. Mater.*, 2017, **29**, 9351–9359.
137 Q. Zhao, W. Huang, Z. Luo, L. Liu, Y. Lu, Y. Li, L. Li, J. Hu, H. Ma and J. Chen, *Sci. Adv.*, 2018, **4**, 1761.